COMMUNICATION

# Remote-controlled regio- and diastereodifferentiating photodimerization of a dynamic helical peptide-bound 2-substituted anthracene†

Received 00th January 20xx,
Accepted 00th January 20xx

DOI: 10.1039/x0xx00000x

Daisuke Taura, Akio Urushima, Yusuke Sugioka, Naoki Ousaka‡ and Eiji Yashima*

**Photodimerization of a novel 2-substituted anthracene linked to a right-handed $3_{10}$-helical nonapeptide induced by long-range chiral information transfer from the remote chiral L-Val residue through a chiral domino effect proceeded in a highly regio- and diastereo-differentiating manner to produce the chiral head-to-head *anti*-photodimer in 90% relative yield with up to 97% diastereomeric excess.**

Remote control of helical chirality through long-range chiral information transfer in dynamic helical systems[1] has recently attracted considerable interest because of its significant degree of chiral amplification of a chiral residue covalently or noncovalently introduced at one chain end of dynamic helical polymers and foldamers, which enables one to induce an excess one-handed helical conformation in a domino-like fashion in spite of achiral majority units in their backbones. This so-called "chiral domino effect"[1a] was first demonstrated using dynamic helical peptides to remote-control its handedness excess[2] and has now been applied to a variety of complex supramolecular chiral systems including the multistep remote-control of the dynamic metal-centered chirality of metallopeptides[3] and planar chirality in metal-bound macrocycles bearing dynamic helical peptides.[4] The chiral domino effect has also been successfully applied to asymmetric reactions[5] catalyzed by a remote catalytic site and diastereoselective reactions that occurred at the termini in a highly stereoselective manner.

On the other hand, we have recently reported the highly diastereo- and enantiodifferentiating [4 + 4] photodimerizations of 2- and 2,6-disubstituted anthracene derivatives that rely on the formations of hetero- and homo-double helices with a controlled handedness induced by a chiral amidine-bound template[6] and amines[7] before photoirradiation, affording the *anti*-head-to-head (HH)- and *anti*-photodimers with up to 88%[6] and 98% enantiomeric excess (ee),[7] respectively. The [4 + 4] asymmetric photodimerizations of substituted anthracenes, in particular, the 2-substituted anthracenes have been thoroughly investigated since the 1980s[8] and almost complete regio-, diastereo- and enantioselective photodimerizations have been achieved using cyclic oligosaccharides, such as γ-cyclodextrin (γ-CyD),[9a] cyclic nigerosylnigerose[9b] and a glucose derivative,[9c] as chiral scaffolds covalently bonded to 2-substituted anthracenes. In these previous examples, however, the use of a stoichiometric quantity of chiral hosts or templates covalently bonded adjacent to the prochiral anthracene units is required to achieve high regio- (head-to-tail (HT) or HH), diastereo- (*anti* or *syn*) and enantioselectivities for the [4 + 4] photodimerization of substituted anthracenes.[10]

Taking advantage of the powerful chiral domino effect on a preferred-handed helix induction of dynamic helical peptides, we envisioned that the photodimerization of a 2-substituted anthracene when linked to a dynamic helical peptide composed of mostly achiral repeating units but with a chiral residue at one chain end would proceed in a highly regio- and diastereo-selective fashion remote-controlled by a one-handed helical peptide induced by long-range chiral information transfer from the remote chiral residue through the chiral domino effect (Fig. 1).

To this end, a novel 2-substituted anthracene derivative (**1**) linked to a dynamic helical nonapeptide with the sequence of –Ac$_6$c-[Api(Boc)-(Ac$_6$c)$_2$]$_2$-L-Val-Aib-OTg

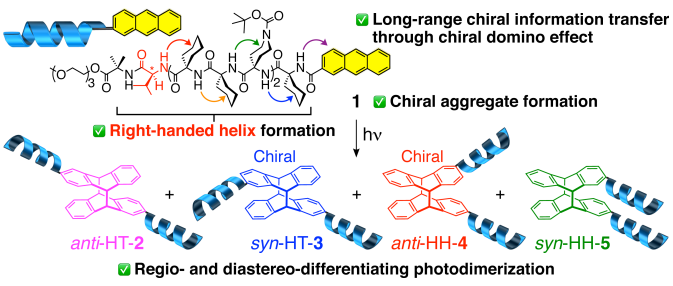


**Fig. 1** Chemical structure of a dynamic helical oligopeptide-bound 2-substituted anthracene (**1**). Schematic illustration for the regio- and diastereo-differentiating photodimerization of **1** assisted by the long-range chiral information transfer from a C-terminal chiral L-Val residue through the covalent-bonding chiral domino effect.

*Department of Molecular and Macromolecular Chemistry, Graduate School of Engineering, Nagoya University, Chikusa-ku, Nagoya 464-8603, Japan. E-mail: yashima@chembio.nagoya-u.ac.jp*

† Electronic supplementary information (ESI) available. Experimental procedures, characterizations of the peptide-bound 2-substituted anthracene (**1**) and its model peptide and additional spectroscopic data. For ESI see DOI: 10.1039/XXXX

‡ Present Address: Molecular Engineering Institute, Kyushu Institute of Technology, Tobata-ku, Kitakyushu, 804-8550, Japan.

(**1**; OTg = 2-(2-(2-methoxyethoxy)ethoxy) ethyl and Boc = *tert*-butoxycarbonyl) was synthesized according to Scheme S1 (ESI†).[11,12] The nonapeptide chain of **1** predominantly formed an excess of a right (*P*)-handed $3_{10}$-helix induced from the remote chiral L-Val residue[14] as revealed by the circular dichroism (CD) spectra of the Z-protected model nonapeptide (Z-Ac$_6$c-[Api(Boc)-(Ac$_6$c)$_2$]$_2$-L-Val-Aib-OTg (**6**); Z = benzyloxycarbonyl) and its molar CD ratio at 223 and 206 nm ($\Delta\varepsilon_{223}/\Delta\varepsilon_{206}$ = 0.33–0.38) measured in $CH_3CN$ (Fig. S3).[3,4,15] The temperature-dependent CD spectral changes of **6** showed that the anisotropic factor at 206 nm ($g_{206} = \Delta\varepsilon_{206}/\varepsilon_{206}$) gradually increased with the decreasing temperature (50 to –20 °C) (Fig. S3a), indicating that the helix-sense excess of the (*P*)-nonapeptide was enhanced at lower temperatures.

The photodimerization of **1** was first investigated in degassed $CD_3CN$ at 25 °C upon light irradiation over 400 nm. The time-dependent $^1$H NMR spectral changes of **1** showed that the peak intensities of the anthracene protons ($H^1$–$H^{10}$) in **1** gradually decreased with time, whereas the cyclodimerized-anthracene and bridge-head ($H^d$ and $H^e$) proton peaks newly appeared at 6.8 − 7.4 and around 4.8 ppm, respectively (Fig. S5a, ESI†), supporting the formation of the [4 + 4] cyclophotodimers.[6]

The four stereoisomers (two achiral *anti*-HT-**2** and *syn*-HH-**5** photodimers and two chiral *syn*-HT-**3** and *anti*-HH-**4** photodimers) (fr.1–fr.5) including one pair of diastereomers (fr.3 and fr.5) were successfully separated and isolated by HPLC with UV and CD dual detectors using $CH_3CN/CH_3OH$ (75/25, (v/v)) as the eluent (see ESI† and Figs. 2a and S12). Another pair of diastereomers (fr.2) was further separated by HPLC into two peaks (fr.2-1 and fr.2-2) with the first positive and second negative CD signs at 300 nm by changing the eluent ($CH_3OH/H_2O$ (95/5, v/v)) (Fig. 2b). The two stereoisomers (fr.1 and fr.4) did not exhibit CD on the HPLC chromatogram and were temporarily assigned to the achiral *syn*-HH-**5** and *anti*-HT-**2** photodimers, respectively (Fig. 2a) based on their $^1$H NMR spectra by comparison with those of the analogous isomers previously reported.[6] In contrast, the two pairs of the isolated diastereomers (fr.3 and fr.5, and fr.2-1 and fr.2-2) showed mirror image CD spectra (Fig. 2c,d), which were then compared to the CD spectra calculated for the (*M*)- or (5*S*,6*S*,11*R*,12*R*)-*syn*-HT- and (*P*)- or (5*R*,6*S*,11*R*,12*S*)-*anti*-HH-photodimers of 2-anthracenecarboxylic acid as the model photodimers of the *syn*-HT-**3** and *anti*-HH-**4** reported by Inoue and co-workers.[16] Consequently, the absolute configurations of the diastereomeric *syn*-HT-**3** (fr.3) and *anti*-HH-**4** (fr.2-1) photodimers were assigned to (*M*) or (5*S*,6*S*,11*R*,12*R*) and (*P*) or (5*R*,6*S*,11*R*,12*S*), respectively. These results suggested that the (*M*)-*syn*-HT-**3** and (*P*)-*anti*-HH-**4** photodimers were predominantly produced when the two anthracene units in **1** are preorganized in the *si–si* HT and *re–re* HH stacked arrangements during the [4 + 4] photodimerization of **1**, respectively, in which the enantioface (*re* or *si*) is defined at the 2-position of the anthracene (Fig. S21, ESI†).

The temperature-dependent CD spectral changes of **1** (50 to –40 °C) in $CH_3CN$ showed split type Cotton effects in the anthracene chromophore region (ca. 230–300 nm) at low

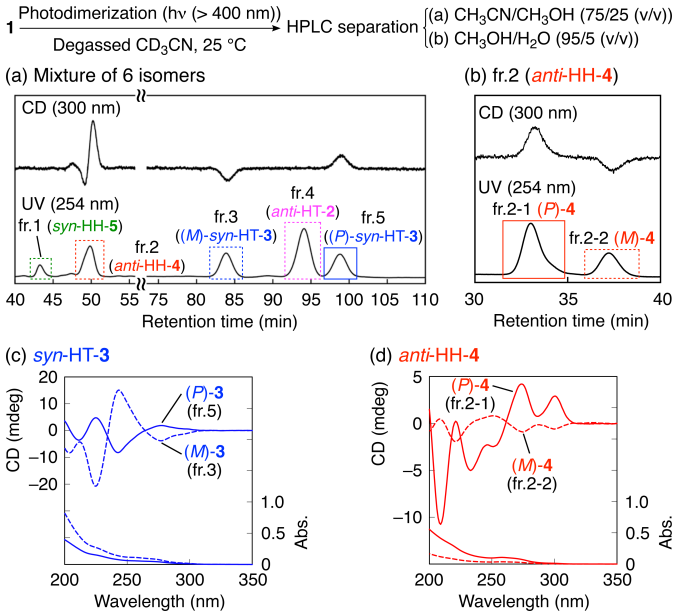


**Fig. 2** (a,b) UV and CD detected HPLC chromatograms of photodimers obtained after light irradiation (> 400 nm) of **1** (0.20 mM) in degassed $CD_3CN$ at 25 °C (run 2, Table 1) (for detail HPLC conditions, see ESI†) (a) and a mixture of (*P*)- and (*M*)-*anti*-HH-**4** (fr.2) (b). (c,d) CD and absorption spectra of (*P*)-*syn*-HT-**3** (c, solid line), (*M*)-*syn*-HT-**3** (c, dotted line), (*P*)-*anti*-HH-**4** (d, solid line) and (*M*)-*anti*-HH-**4** (d, dotted line) in $CH_3OH$ at 25 °C. The two achiral photodimers (*anti*-HT-**2** (fr.4) and *syn*-HH-**5** (fr.1)) were temporarily assigned on the basis of the $^1$H NMR spectra of the analogous isomers reported previously.[6]

temperatures and the CD intensities increased with the decreasing temperature (Fig. 3a). These results suggest a chiral aggregate formation of the anthracene units of **1**, in which the two anthracene units are helically stacked with an excess twist-sense at low temperatures assisted by the $3_{10}$-(*P*)-helical nonapeptide with an excess of one-handedness biased by the remote chiral L-Val residue.

The photodimerizations of **1** in degassed $CD_3CN$ (0.20 mM) at various temperatures (50, 25, 0, –10, –20 and –40 °C) were next investigated (runs 1–4, 6 and 8 in Table 1). Based on the time-dependent $^1$H NMR spectral changes, the conversions and the first-order rate constants ($k$) for the photodimerizations of **1** at different temperatures were estimated to be 75 – 87% and $0.22 \times 10^{-3}$ – $0.31 \times 10^{-3}$ $s^{-1}$, respectively (Figs. S4–S7, S9 and S11, ESI† and Table 1). The photoirradiations of **1** at 50 and 25 °C proceeded in an HT-selective manner (HT/HH = 81/19 and 77/23), giving the chiral *syn*-HT-**3** photodimer in 38 and 37% relative yields with no diastereoselectivity together with the chiral *anti*-HH-**4** photodimer in 15 and 18% relative yields with +24 and +41% diastereomeric excess (de), respectively (runs 1 and 2 in Table 1 and Figs. 2a, 3b and S12a, ESI†). Moreover, the relative yields of the chiral *anti*-HH-**4** photodimer and its diastereoselectivities were modestly enhanced to 30 and 41%, and +62 and +74% de at 0 and –10 °C, respectively (runs 3 and 4 in Table 1 and Figs. 3b and S12b,c, ESI†). Interestingly, the relative yield of the *anti*-HH-**4** and its diastereoselectivity were significantly improved to 58% and +86% de at –20 °C and further remarkably enhanced to ca. 90% and +97% de at –40 °C, respectively, thus selectively producing the HH-photodimer

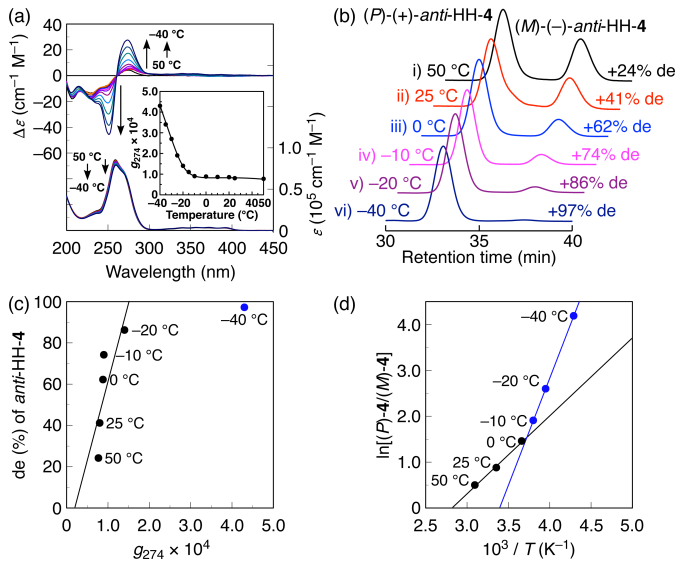


**Fig. 3** (a) Temperature-dependent CD and absorption spectral changes of **1** in $CH_3CN$ (0.20 mM). Inset shows the plots of the *g*-value ($\Delta\varepsilon_{274}/\varepsilon_{274}$) of **1** at 274 nm ($g_{274}$) versus temperature. The solid line is drawn to guide the eyes. (b) UV detected (254 nm) HPLC chromatograms for the separation of the diastereomers of (*P*)-(+)- and (*M*)-(–)-*anti*-HH-**4** obtained by the photodimerizations of **1** in $CD_3CN$ at various temperatures. + and – denote the signs of the Cotton effect at 300 nm corresponding to the *P* and *M* diastereomers, respectively. (c) Relationships between the *g*-value ($\Delta\varepsilon_{274}/\varepsilon_{274}$) of **1** at 274 nm ($g_{274}$) measured at various temperatures and the corresponding de (%) values of the *anti*-HH-**4** produced at those temperatures after photoirradiation of **1**. The *g* and de (%) values are taken from Fig. 3a,b and Table 1. (d) Plots of the natural logarithm of the diastereomeric ratio of (*P*)- and (*M*)-*anti*-HH-**4** ([(*P*)-**4**]/[(*M*)-**4**]) against the reciprocal temperature upon photoirradiation of **1** (data are taken from runs 1–4, 6 and 8, Table 1).

(HT/HH = ca. 9/91) with an excellent diasetereoselectivity at –40 °C (runs 6 and 8 in Table 1 and Figs. 3b and S12d,e, ESI†).[17] On the other hand, the diastereoselectivity of the chiral *syn*-HT-**3** was quite low (–3 – –7% de) within the temperature range of 0 to –20 °C (runs 3, 4 and 6 in Table 1 and Fig. S12, ESI†).

The observed temperature-dependent enhancement of the diastereoselectivity of the *anti*-HH-**4** was mostly correlated with the induced CD intensity of the terminal anthracene unit of **1**, which was significantly increased at low temperatures before the photoirradiation. The *g*-values ($g_{274}$) of **1** at various temperatures were then plotted as a function of the diastereoselectivities (% de values) of the chiral *anti*-HH-**4** photodimer produced during the photoirradiations of **1** at those temperatures, giving an almost linear relationship except for the result performed at –40 °C (Fig. 3c). As a result, the diastereoselectivity of the chiral *anti*-HH-**4** photodimer tended to increase as the *g*-value ($g_{274}$) increased with the decreasing temperature.

In order to further discuss the temperature effect on the predominant formation of the chiral *anti*-HH-**4** photodimer during the regio- and diastereoselective photodimerizations of **1**, the natural logarithms of the HT/HH ratio and relative rate constant ($\ln(k_+/k_-)$) for producing the (*P*)-(+)- and (*M*)-(–)-*anti*-HH-**4** photodimers, respectively, calculated from their relative diastereomer ratios ($k_+/k_-$ = (100 + de%)/(100 – de%) = (*P*)-**4**/(*M*)-**4**) were plotted versus the reciprocal temperature ($1/T$) within the temperature range of 50 to –40 °C. The both plots were discontinuous at around 0 – –10 °C that likely gave two straight lines, suggesting two mechanisms that took place depending on the temperature (Figs. 3d and S12f, ESI†). A kind of supramolecular aggregate formation between the terminal anthracene units of **1** at the low temperatures probably below –10 °C may be taken into consideration based on the temperature-dependent CD intensity changes (Fig. 3a). The temperature-dependent $^1$H NMR spectral changes of **1** measured in $CD_3CN$ at – 40 – 50 °C (Fig. S18, ESI†) suggested the formation of aggregates of **1**, showing broad but largely separated sets of new aromatic proton signals with significant upfield shifts at low temperatures (< –20 °C). The observed remarkable enhancements of the relative yield of the chiral *anti*-HH-**4** photodimer and its diastereoselectivity at low temperatures may be explained by the helically-stacked prochiral anthracene units of **1** preorganized to form a *re–re* stacked manner, resulting in the formation of the (*P*)-(+)-*anti*-HH-**4** photodimer.

The photodimerization of **1** was then performed in degassed $CD_3CN$ at a higher concentration (1.0 mM) and low temperature (–10 and –20 °C). As expected, the relative yields of the chiral *anti*-HH-**4** photodimer and their de values were slightly improved to 45 and 63%, and +81 and +88% de at –10 and –20 °C,[18] respectively, indicating the role of the chiral aggregate formation (runs 5 and 7 in Table 1). Obviously, further experiments will be needed to elucidate the structure of such a supramolecular aggregate in solution.

**Table 1** Results of photodimerizations of **1** (0.20 mM) in degassed $CD_3CN$ at various temperatures upon light irradiation over 400 nm for 120 min

| Run | Temp. (°C) | $g_{274} \times 10^3$[a] | Conv. (%)[b] (Consumption rate $10^{-3}$ $k$ ($s^{-1}$)) | Relative yield (%) (de (%))[c] | | | | Ratio |
|---|---|---|---|---|---|---|---|---|
| | | | | *anti*-HT-**2** | *syn*-HT-**3** | *anti*-HH-**4** | *syn*-HH-**5** | HT/HH |
| 1 | 50 | +0.077 | 87 (0.31) | 43 | 38 (0) | 15 (+24) | 4 | 81/19 |
| 2 | 25 | +0.080 | 83 (0.28) | 40 | 37 (0) | 18 (+41) | 5 | 77/23 |
| 3 | 0 | +0.088 | 78 (0.23) | 35 | 30 (–3) | 30 (+62) | 5 | 65/35 |
| 4 | –10 | +0.090 | 79 (0.23) | 29 | 25 (–4) | 41 (+74) | 5 | 54/46 |
| 5[d] | –10 | +0.24 | 84 (0.28) | 27 | 24 (–4) | 45 (+81) | 4 | 51/49 |
| 6 | –20 | +0.14 | 76 (0.22) | 21 | 17 (–7) | 58 (+86) | 4 | 38/62 |
| 7[d] | –20 | +0.39 | 75 (0.19) | 21 | 14 (–22) | 63 (+88) | 2 | 35/65 |
| 8 | –40 | +0.43 | 75 (0.22) | ~7 | < 2 (–)[e] | ~90 (+97) | < 1 | ~9/91 |

[a] The *g*-value ($\Delta\varepsilon_{274}/\varepsilon_{274}$) of **1** at 274 nm in $CH_3CN$. [b] Estimated by $^1$H NMR. [c] Determined by HPLC (see Figs. 2a,b, 3b and S12, ESI†). + and – denote the signs of the Cotton effect at 300 nm corresponding to the *P* and *M* diastereomers, respectively. [d] [**1**] = 1.0 mM. [e] Not determined due to poor yield.

In conclusion, we have achieved the highly regio- and diastereo-differentiating photodimerization of a right-handed $3_{10}$-helical nonapeptide-bound 2-anthracene derivative (**1**), in which the chiral *anti*-HH-photodimer (*anti*-HH-**4**) was produced as the main product in ca. 90% relative yield with up to 97% diastereomeric excess in $CD_3CN$ at low temperature. The remarkable temperature effect on the formation of the *anti*-HH-photodimer along with its significant enhancement of its diastereoselectivity was observed, which may rely on the chiral covalent domino effect followed by a supramolecular aggregation of the anthracene residues. The present findings will be further applied to the development of a unique supramolecular asymmetric photoreaction system in water since the Boc groups of **1** can be readily deprotected to afford a water-soluble 2-anthracene-bound helical peptide,[12] which may assemble with achiral anthracene derivatives bearing achiral, but dynamically racemic helical peptide chains in water to form supramolecular helical hetero-aggregates with amplification of the chirality,[1d,19] leading to a more efficient regio-, diastereo- and/or enantiodifferentiating photodimerization in the presence of a catalytic amount of the water-soluble 2-anthracene-bound helical peptide. Work along this line is now in progress in our laboratory.

This work was supported by JSPS KAKENHI (Grant-in-Aid for Specially Promoted Research, no. 18H05209 (E.Y.) and Grant-in-Aid for Scientific Research (C), no. 18K05059 (D.T.)).

## Conflicts of interest

There are no conflicts to declare.

## Notes and references


1 (a) Y. Inai, H. Komori and N. Ousaka, *Chem. Rec.*, 2007, **7**, 191–202; (b) M. Crisma, M. De Zotti, F. Formaggio, C. Peggion, A. Moretto and C. Toniolo, *J. Pept. Sci.*, 2015, **21**, 148–177; (c) B. A. F. Le Bailly and J. Clayden, *Chem. Commun.*, 2016, **52**, 4852–4863; (d) E. Yashima, N. Ousaka, D. Taura, K. Shimomura, T. Ikai and K. Maeda, *Chem. Rev.*, 2016, **116**, 13752–13990.

2 For examples of domino-type chiral information transfer along achiral, but dynamic helical peptide and polymer backbones, see: (a) E. Benedetti, A. Bavoso, B. Di Brasio, V. Pavone, C. Pedone, C. Toniolo and G. M. Bonora, *Proc. Natl. Acad. Sci. USA.*, 1982, **79**, 7951–7954; (b) Y. Okamoto, M. Matsuda, T. Nakano and E. Yashima, *Polym. J.*, 1993, **25**, 391–396; (c) Y. Inai, K. Tagawa, A. Takasu, T. Hirabayashi, T. Oshikawa and M. Yamashita, *J. Am. Chem. Soc.*, 2000, **122**, 11731–11732; (d) Y. Inai, Y. Ishida, K. Tagawa, A. Takasu and T. Hirabayashi, *J. Am. Chem. Soc.*, 2002, **124**, 2466–2473; (e) J.-P. Mazaleyrat, K. Wright, A. Gaucher, N. Toulemonde, M. Wakselman, S. Oancea, C. Peggion, F. Formaggio, V. Setnička, T. A. Keiderling and C. Toniolo, *J. Am. Chem. Soc.*, 2004, **126**, 12874–12879; (f) J. Clayden, A. Castellanos, J. Solà and G. A. Morris, *Angew. Chem., Int. Ed.*, 2009, **48**, 5962–5965; (g) K. Maeda, S. Wakasone, K. Shimomura, T. Ikai and S. Kanoh, *Chem. Commun.*, 2012, **48**, 3342–3344; (h) R. A. Brown, V. Diemer, S. J. Webb and J. Clayden, *Nat. Chem.*, 2013, **5**, 853–860; (i) M. D. Poli, W. Zawodny, O. Quinonero, M. Lorch, S. J. Webb and J. Clayden, *Science*, 2016, **352**, 575–580; (j) F. G. A. Lister, B. A. F. Le Bailly, S. J. Webb and J. Clayden, *Nat. Chem.*, 2017, **9**, 420–425.

3 N. Ousaka, Y. Takeyama, H. Iida and E. Yashima, *Nat. Chem.*, 2011, **3**, 856–861.

4 F. Mamiya, N. Ousaka and E. Yashima, *Angew. Chem., Int. Ed.*, 2015, **54**, 14442–14446.

5 (a) L. Byrne, J. Solà, T. Boddaert, T. Marcelli, R. W. Adams, G. A. Morris and J. Clayden, *Angew. Chem., Int. Ed.*, 2014, **53**, 151–155; (b) L. Byrne, J. Solà and J. Clayden, *Chem. Commun.*, 2015, **51**, 10965–10968; (c) J. Maury, B. A. F. Le Bailly, J. Raftery and J. Clayden, *Chem. Commun.*, 2015, **51**, 11802–11805; (d) B. A. F. Le Bailly, L. Byrne and J. Clayden, *Angew. Chem., Int. Ed.*, 2016, **55**, 2132–2136; (e) D. Mazzier, M. Crisma, M. D. Poli, G. Marafon, C. Peggion, J. Clayden and A. Moretto, *J. Am. Chem. Soc.*, 2016, **138**, 8007–8018.

6 J. Tanabe, D. Taura, N. Ousaka and E. Yashima, *J. Am. Chem. Soc.*, 2017, **139**, 7388–7398.

7 A. Urushima, D. Taura, M. Tanaka, N. Horimoto, J. Tanabe, N. Ousaka, T. Mori and E. Yashima, *Angew. Chem., Int. Ed.*, 2020, **59**, 7478–7486.

8 (a) T. Tamaki, *Chem. Lett.*, 1984, **13**, 53–56; (b) N. Vallavoju and J. Sivaguru, *Chem. Soc. Rev.*, 2014, **43**, 4084–4101; (c) C. Yang and Y. Inoue, *Chem. Soc. Rev.*, 2014, **43**, 4123–4143; (d) V. Ramamurthy and J. Sivaguru, *Chem. Rev.*, 2016, **116**, 9914–9993.

9 (a) C. Yang, C. F. Ke, W. T. Liang, G. Fukuhara, T. Mori, Y. Liu and Y. Inoue, *J. Am. Chem. Soc.*, 2011, **133**, 13786–13789; (b) G. Fukuhara, T. Nakamura, Y. Kawanami, C. Yang, T. Mori, H. Hiramatsu, Y. Dan-oh, T. Nishimoto, K. Tsujimoto and Y. Inoue, *J. Org. Chem.*, 2013, **78**, 10996–11006; (c) G. Fukuhara, K. Iida, Y. Kawanami, H. Tanaka, T. Mori and Y. Inoue, *J. Am. Chem. Soc.*, 2015, **137**, 15007–15014. For highly enantiodifferentiating photodimerization of 2-anthracenecarboxylic acid mediated by liquid crystal phases, see: (d) Y. Ishida, Y. Kai, S.-y. Kato, A. Misawa, S. Amano, Y. Matsuoka and K. Saigo, *Angew. Chem., Int. Ed.*, 2008, **47**, 8241–8245; (e) Y. Ishida, Y. Matsuoka, Y. Kai, K. Yamada, K. Nakagawa, T. Asahi and K. Saigo, *J. Am. Chem. Soc.*, 2013, **135**, 6407–6410.

10 Inoue and co-workers reported the first catalytic photodimerization of 2-anthracenecarboxylic acid in the presence of a catalytic amount of diamino-γ-CyD with an excess amount of $Cu^{2+}$ ions in an aqueous solution, giving the *anti*-HH photodimer of 70% ee in 52% relative yield. See: C. F. Ke, C. Yang, T. Mori, T. Wada, Y. Liu and Y. Inoue, *Angew. Chem., Int. Ed.*, 2009, **48**, 6675–6677.

11 A. Urushima, N. Ousaka and E. Yashima, *Chem. Asian J.*, 2018, **13**, 3150–3154.

12 1-Aminocyclohexane-1-carboxylic acid ($Ac_6c$), 1-aminopiperidine-1-carboxylic acid (Api) and α-aminoisobutyric acid (Aib) are known as strong helicogenic achiral $C^{\alpha}$-tetrasubstituted α-amino acids that form a stable $3_{10}$-helix.[13] The Api moieties were employed for further applications to develop a water-soluble helical peptide after deprotection of the Boc groups of **1**.

13 (a) C. Toniolo, M. Crisma, F. Formaggio and C. Peggion, *Biopolymers*, 2001, **60**, 396–419; (b) C. Tonlolo and E. Benedetti, *Trends Biochem. Sci.*, 1991, **16**, 350–353.

14 The (*P*)-$3_{10}$-helical structure of **1** was stabilized by intramolecular hydrogen-bond networks along the peptide chain as supported by the 2D ROESY NMR (Figs. S15 and S16, ESI†) and temperature-dependent $^1$H NMR (Fig. S20a, ESI†) measurement results.

15 C. Toniolo, A. Polese, F. Formaggio, M. Crisma and J. Kamphuis, *J. Am. Chem. Soc.*, 1996, **118**, 2744–2745.

16 A. Wakai, H. Fukasawa, C. Yang, T. Mori and Y. Inoue, *J. Am. Chem. Soc.*, 2012, **134**, 4990–4997.

17 Inversion of the HT/HH ratio of 2-substituted anthracene derivatives during the photodimerization remains rare, see: (a) A. Nakamura and Y. Inoue, *J. Am. Chem. Soc.*, 2005, **127**, 5338–5339; (b) C. Yang, T. Mori, Y. Origane, Y. H.-Ko, N. Selvapalam, K. Kim and Y. Inoue, *J. Am. Chem. Soc.*, 2008, **130**, 8574–8575; (c) J. B. Yao, Z. Q. Yan, J. C. Ji, W. H. Wu, C. Yang, M. Nishijima, G. Fukuhara, T. Mori and Y. Inoue, *J. Am. Chem. Soc.*, 2014, **136**, 6916–6919.

18 Because of the low solubility of **1** in $CD_3CN$, the photodimerization at lower temperatures was difficult.

19 (a) A. R. A. Palmans and E. W. Meijer, *Angew. Chem., Int. Ed.*, 2007, **46**, 8948–8968; (b) M. Liu, L. Zhang and T. Wang, *Chem. Rev.*, 2015, **115**, 7304–7397.


 

Graphical abstract

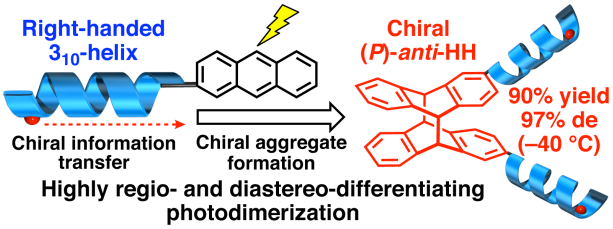


Photodimerization of a right-handed $3_{10}$-helical nonapeptide-bound 2-substituted anthracene produced the chiral head-to-head *anti*-photodimer with up to 97% diastereomeric excess.